Using the *aa* index over the last 14 solar cycles to characterize extreme geomagnetic activity.

S. C. Chapman[1], R. B. Horne[2], and N. W. Watkins[1,3,4]

[1]Centre for Fusion, Space And Astrophysics, Physics Department, University of Warwick, Coventry CV4 7AL
[2]British Antarctic Survey, Cambridge, CB3 0ET, UK
[3]Centre for the Analysis of Time Series, London School of Economics and Political Science, London, WC2A 2AZ, UK
[4]Faculty of Science, Technology, Engineering and Mathematics, The Open University, Milton Keynes, UK

Key Points:

- We present a new method that parameterizes extremes of 14 solar cycles of the aa geomagnetic index
- We find a 4% (28%) chance of at least one great (severe) storm per year over 14 solar cycles
- A D_{ST} weaker than $-1000nT$ Carrington storm is in the same occurrence rate distribution as other super-storms since 1868

Corresponding author: S. C. Chapman, S.C.Chapman@warwick.ac.uk

This article has been accepted for publication and undergone full peer review but has not been through the copyediting, typesetting, pagination and proofreading process which may lead to differences between this version and the Version of Record. Please cite this article as doi: 10.1029/2019GL086524

Abstract

Geomagnetic indices are routinely used to characterize space weather event intensity. The D_{ST} index is well resolved, but is only available over 5 solar cycles. The *aa* index extends over 14 cycles but is highly discretized with poorly resolved extremes. We parameterize extreme *aa* activity by the annual averaged top few % of observed values, show these are exponentially distributed and they track annual D_{ST} index minima. This gives a 14 cycle average of $\sim 4\%$ chance of at least one great ($D_{ST} < -500nT$) storm and $\sim 28\%$ chance of at least one severe ($D_{ST} < -250nT$) storm per year. At least one $D_{ST} = -809$ $[-663, -955]nT$ event in a given year would be a 1:151 year event. Carrington event estimate $D_{ST} \sim -850nT$ is within the same distribution as other extreme activity seen in *aa* since 1868 so that its likelihood can be deduced from that of more moderate events. Events with $D_{ST} \lesssim -1000nT$ are in a distinct class, requiring special conditions.

Plain Language Summary

Here we use measurements of disturbances in the Earth's magnetic field that go back to 1868, and we present a novel way of analysing the data to identify the largest magnetic storms going back some 80 years longer than has been done before. As a result, we are able to state the chance of at least one super-storm occurring in a year. We find that on average there is a 4% (28%) chance of at least one great (severe) storm per year, and a 0.7% chance of a Carrington class storm per year, which can be used for planning the level of mitigation needed to protect critical national infrastructure.

1 Introduction

Extreme space weather events significantly disrupt systems for power distribution, aviation, communication and satellites; they are driven by large scale plasma structures emitted from the solar corona but their impact depends on a variety of factors [Baker & Lanzerotti, 2016]. Quantifying the chance of occurrence of extreme space weather events is essential to planning the resilience of vulnerable systems to catastrophic failure. Events that lead to geomagnetically induced currents that affect power grids are more likely close to solar maximum and in the descending phase of the solar cycle, but importantly they can occur at all other times in the solar activity cycle [Thomson et al., 2010]. The number of major solar eruptions varies with the approximately 11 year cycle of solar (sunspot) activity and with the amplitude of each solar cycle which is unique [Hathaway, 2015]. A particular concern is the possibility of a Carrington-class event, named after the space weather super-storm of 1859 [Tsurutani et al., 2003; Cliver & Svalgaard, 2004; Cliver & Dietrich, 2013] which today could arguably cause severe disruption [Cannon et al., 2013; Daglis, 2004; Oughton et al., 2017].

Due to their rarity, amplitude and occurrence rates of space weather super-storms are challenging to quantify; it requires modelling based on the few observed large events. There have been a number of statistical studies, most of which rely on observations since the beginning of the space age. Estimates based on extrapolating a power law event distribution [Riley, 2012] suggest a 12% probability of a Carrington-class event in any given solar cycle, but are highly uncertain [Riley & Love, 2016]. A log-normal event distribution yields a much lower probability, again with a wide confidence interval [Love et al., 2015]. Estimates based on Extreme Value Theory [Thomson et al., 2011] also suggest the probability can be much lower [Siscoe, 1976; Silbergleit, 1996, 1999; Tsubouchi & Omura, 2007; Elvidge & Angling, 2018]. More moderate storms provide a larger set of observations. When storms across different solar cycles are aggregated, there is a well established correlation between occurrence rate and solar activity [Tsurutani et al., 2006; Tsubouchi & Omura, 2007]. Both solar wind driving [Tindale & Chapman, 2016, 2017] and geomagnetic activity [Hush et al., 2015; Chapman et al., 2018; Lockwood et al., 2018a]

track the differences in the level of activity at different phases of distinct solar cycles, and between cycles of different intensity.

The above statistical studies are feasible for indices which are well resolved in amplitude, such as D_{ST}. Whereas most indices, such as D_{ST}, are only available over the last 5 solar cycles, the *aa* index extends across 14 solar cycles- it is the longest almost continuous record of changes in magnetic field across the earth's surface. Given the variability in the amplitude of different solar cycles, it is desirable to obtain event occurrence rates for this longer sample. However the *aa* index is by construction based on combining observations that are logarithmically discretized in amplitude and thus individual records of the 3 hour *aa* index will have uncertainties that are both significant and non-trivial to estimate [Bubenik & Fraser-Smith, 1977].

In this Letter we propose a parameterization of extreme *aa* activity using averages of the annual top few % of observed records. Our goal is to use *aa* to obtain a proxy for D_{ST} extremes that have occurred over the last 150 years. Our methodology is as follows. We first show that there is a good linear correlation between the annual average of the top few % values of *aa* and the annual D_{ST} minimum seen over the last 5 solar cycles. This establishes a linear 'mapping' between the annual average of the top few % values of *aa* and the annual D_{ST} minimum. We next use this linear mapping to convert these 150 annual averages of the top few % of *aa* values into proxy D_{ST} extremes. This gives us 150 estimates for the annual minimum D_{ST} that occurred over the last 14 solar cycles of activity. This record then provides an estimate of how many years have included super-storm activity over the last 14 cycles, where super-storm activity is categorised in terms of the largest annual event crossing a typical threshold minimum D_{ST} level. We find that the largest samples are exponentially distributed. We can then determine the range of minimum D_{ST} that would occur if this distribution applied to the next largest record in excess of these 150 estimates, that is, a 1:151 year event. The Carrington event is also characterised in terms of its excursion in D_{ST} and estimates vary considerably [Tsurutani et al., 2003; Siscoe et al., 2006; Hayakawa et al., 2019]. We compare these estimates with the range of minimum D_{ST} for a 1:151 event inferred from the 14 solar cycle proxy D_{ST} extremes record. This provides an assessment of whether the Carrington event was a more intense version of the other super-storms that have occurred since 1868 or whether it was in a class of its own, which would require the concurrence of special conditions in the corona and solar wind and at the earth. Only if it is the former can we use the set of observed storms to try to predict how likely such an event is in the future.

2 The datasets

Geomagnetic indices are derived from ground based magnetometer observations [Mayaud, 1980] and are widely used to indicate the intensity of space weather events. The D_{ST} index [Sugiura, 1964; Sugiura & Kamei, 1991] measures low-latitude global variations in the horizontal component of the geomagnetic field, thus representing the strength of the equatorial ring current. The D_{ST} index is available [WDC, 2015] since 1957, so that we can directly compare the *aa* index to D_{ST} over the last 5 solar cycles.

We focus on the 3-hourly resolution *aa* index over the last 14 solar cycles, from 1868 to the present. This will be analysed alongside the daily sunspot number which is available for the same time period. The *aa* index is constructed [Mayaud, 1972] from the *K* indices determined at two antipodal observatories (invariant magnetic latitude 50 degrees) to provide a quantitative characterization of magnetic activity, which is homogeneous through the whole series. A key consideration for this study is that the *aa* index (units, *nT*) is discretized in amplitude [Bubenik & Fraser-Smith, 1977] since the underlying *K* index [Bartels et al., 1939] is a quasi-logarithmic 0-9 integer scale that characterizes the maximum positive and negative magnetic deviations that occur during each 3 hour period at a given observatory. Due to its longevity, the index has also recently required

some corrections. The response seen by a magnetometer to geomagnetic activity depends on the station's location wrt the auroral oval. A scale-factor for each station is applied to the scale of threshold values used to convert the observed continuous values into quantized K values. This scale factor is adjusted for each station to allow for its location and characteristics such that the K value is a standardized measure of the level of geomagnetic activity, irrespective of the location of the observation. The Mayaud [1980] original scheme assumes that this scale factor does not change with time. This does not account for secular changes in the intrinsic geomagnetic field that have occurred over the 150 years of the *aa* index, which introduce a drift in the individual stations and 'steps' in value as stations are changed. These are discussed in detail, and corrected for in Lockwood et al. [2018b]. These corrections are typically less than $10nT$ in magnitude and whilst this is important for estimates of the overall long term change in *aa*, it is a relatively small (and we will see, within uncertainties) perturbation on typical super-storm values. Lockwood et al. [2018c] extended this work to correct for hemispheric asymmetry using a model of the time-of-year and time-of-day response functions of the stations. They have produced a homogenized 3-hourly *aa* index utilizing these corrections. We have repeated the analysis here for both the homogenized and original ('classic') versions of the *aa* index and key plots that use the homogenized *aa* index in the main sections of the Letter are reproduced using the 'classic' (ISGI) *aa* index in the SI. The homogenized *aa* index is available to end 2017 and our analysis extends up to this date, giving 150 calendar years of data.

3 The *aa* index compared to D_{ST} at large values

As the *aa* index is non-linearly and non-uniformly discretized in amplitude, we need to explore to what extent it can be used to characterize super-storms. We can see this by comparing it to $(-)D_{ST}$, which is a well established measure of geomagnetic storm intensity. The D_{ST} index is well sampled in amplitude and therefore its maximum value does provide a meaningful estimate of super-storm intensity. Semilog rank order plots [Sornette, 2003] provide a method to display the behaviour of a set of values, particularly where they are large to extreme. The observations x_k are sorted in descending amplitude and plotted (ordinate) versus their rank k (abscissa), that is, the largest observed value is rank 1, the next largest, rank 2 and so on. Figure 1 compares rank order plots of the data records for $(-)D_{ST}$ with that for classic and homogenized *aa* for the solar maximum interval, the solar minimum interval, and the declining phase of each of the last five solar cycles for which D_{ST} is avaiable. We identify the intervals of solar minimum, solar maximum and the declining phases by applying a single algorithm across the entire time series as detailed in the SI. In Figure 1 it is immediately apparent that the classic *aa* amplitude is strongly discretized at the high values, whereas $(-)D_{ST}$ resolves them. Figure 1 plots the individual data points and the homogenized *aa* index shown in Figure 1 (d,e,f) is less discretized in appearance [Lockwood et al., 2018c] than the classic *aa* as the individual datapoints have been adjusted using time and station dependent scale factors as discussed above. Whilst this does correct *aa* for secular changes, it cannot recover the information lost by the original discretization, on a quasi-logarithmic scale, involved in constructing the K indices that underlie the *aa* index. Therefore the *aa* maximum value (within a given interval, or event) does not quantify the extrema of geomagnetic disturbances very well. As a consequence, *aa* is not readily amenable to standard analysis techniques for extracting, and quantifying the statistical properties of events or bursts. Thus whilst the Peak Over Threshold (POT) method has been successfully applied in quantifying the statistics of events in D_{ST} using Extreme Value Theory (e.g. [Tsubouchi & Omura, 2007]) it cannot simply be applied to the *aa* index. For this reason we will focus on year-long averages of the largest 0.5% and 5% *aa* records seen in each year as an estimate of the relative level of extreme activity captured by the *aa* index. Figure 1 verifies that the large *aa* and $(-)D_{ST}$ records do indeed both follow the variation within and between solar cycles in the same manner despite the discretization present in the *aa* index. We can hence use *aa* to

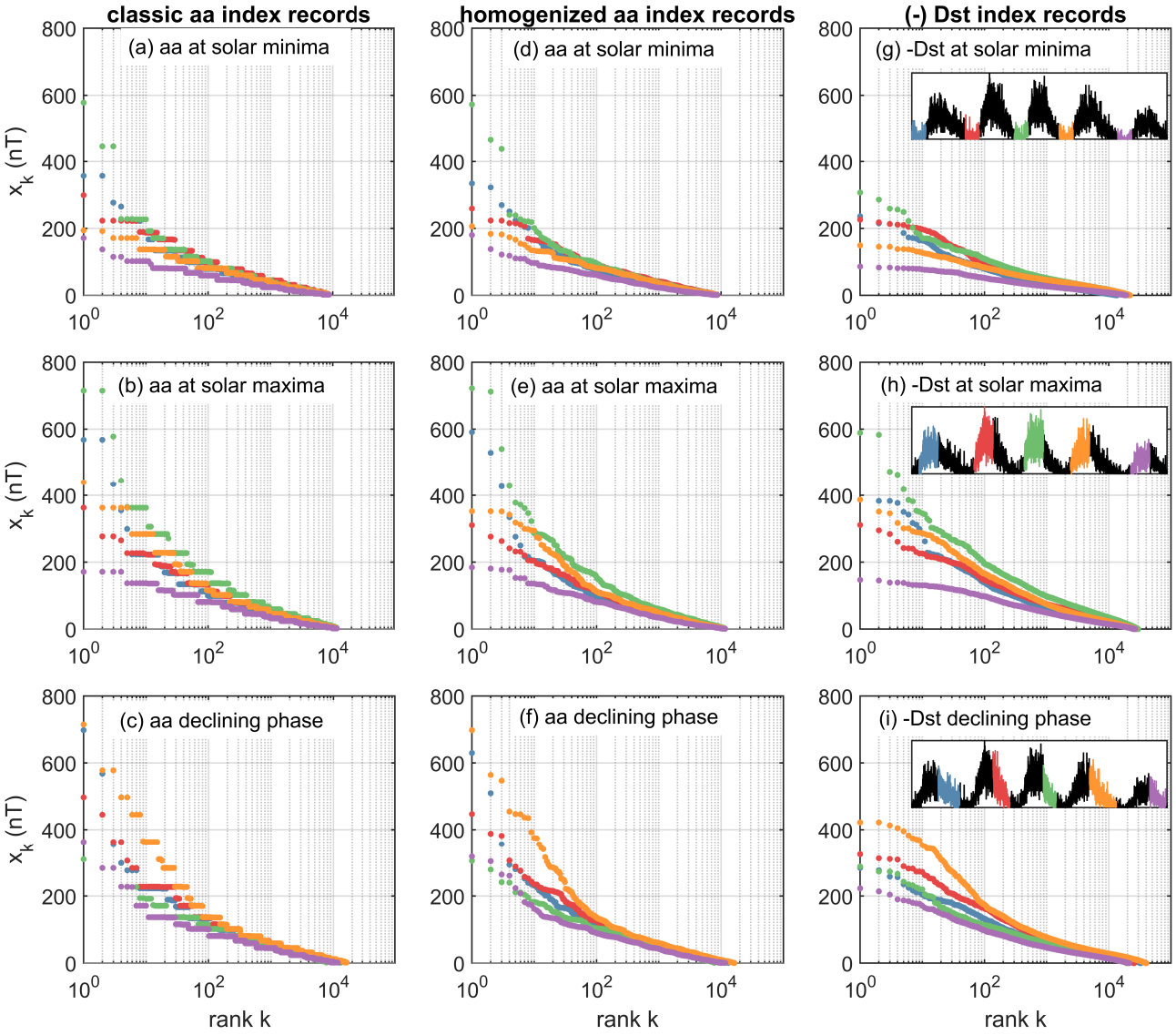

Figure 1. Rank order plots at the minima, maxima and declining phases of the last five solar cycles plotting data records for the classic *aa* index (a,b,c), the homogenized [Lockwood et al., 2018b,c] *aa* index (d,e,f) and $-D_{ST}$ index (g,h,i). The time interval from which data is used to form each rank order plot is indicated in the inset, overplotted on the daily sunspot number. Colours indicate the solar cycle 20 (blue) 21 (red) 22 (green) 23 (orange) 24 (purple).

provide an indication of the variation in the extremes of geomagnetic activity over the last 14 solar cycles.

4 Historical space weather activity

Figure 2 plots the level of extreme activity captured by the homogenized *aa* index versus annual average sunspot number from 1868-2017 inclusive, corresponding to the last 14 solar cycles. We parameterize extreme activity in *aa* by annual averages of the largest 0.5 % (top panels), the largest 5 % (centre panels), and compare this with the average of all records (bottom panels). The averages are performed over non-overlapping calendar years. The left hand panels (a,b,c) of Figure 2 show the parameter space explored by *aa* and sunspot number over the last 14 solar cycles. Fig 2 (c) reproduces the well known result [Feynman, 1982] that time *averages* of *aa* always exceed a baseline value which increases linearly with averaged sunspot number. A baseline can also be seen in the annual averages of the largest 0.5 % and the largest 5 % *aa* values.

We use the data from the last 5 solar cycles to obtain an approximate mapping between values of extreme activity in D_{ST} and *aa* parameterized as above. We expect from Figure 1 that the large to extreme records of *aa* will track those of D_{ST}. As discussed above, the amplitude of D_{ST} is well resolved, so that we can consider the single observed minimum D_{ST} record that occurs in any given calendar year as a measure of the most severe storm that occurred in that year. Figure 3 overplots versus time the non-overlapping calendar year annual averages of the largest 0.5 % of the homogenized *aa* index with the maximum of (-) D_{ST} that occurs in the same calendar year. We see that these quantities do track each other, albeit imperfectly. Figure 2, panel (d) plots (blue dots) these same quantities against each other, that is, the non-overlapping calendar year annual averages of the largest 0.5 % of the homogenized *aa* index are plotted versus the maximum of (-) D_{ST} that occurs in each calendar year as a scatter plot. Figures 2 (e,f) plot the analogous scatter plots for annual averages of the largest 5 %, and annual averages of *aa*. Since the *aa* index is derived from observatory *K* index values it has an upper bound, whereas D_{ST} is unbounded. If the observed values of *aa* over the last five solar cycles (where we have contemporaneous D_{ST}) explored this upper bound, we would see a saturation or 'pile up' in *aa* when plotted versus D_{ST}. We do not see any evidence of saturation in Figure 2 (d,e) and therefore perform a least squares linear regression fit which is plotted as the solid black line, the .95 confidence bounds are indicated by dotted lines. The r-squared coefficient of determination (which indicates the proportionate amount of variation in the response variable explained by the variable in the linear regression model) for each fit is given on the panels. Non-overlapping calendar year annual averages of the largest 0.5 % of the homogenized *aa* index (panel d) are well described by the linear least squares fit to annual minimum D_{ST} with r-squared coefficient of determination $r = 0.81$. The coefficients of this fitted line $a(x - b)$ are (with 95% confidence intervals) $a = 0.87$ $[0.76, 0.99]$ and $b = -43.12$ $[-79.48, -6.76]$. The fit is reasonable, $r = 0.76$ for the largest 5 % (panel e). We need to choose a high threshold in order to isolate the largest events seen in each year of the *aa* index in order for these to be comparable with the largest annual minimum value of the D_{ST} index. This confirms that the correspondence is not strongly sensitive to the particular choice of high threshold. As we would expect, the correspondence will be poor between the annual averages of *aa* and the largest annual minimum of D_{ST} and this is indeed the case with $r = 0.4$ (panel f). We therefore focus on the annual averages of the largest few % of the *aa* index as the parameter for extreme activity.

We now use this least squares fit to read across between annual averages of the largest few % of *aa* records to the corresponding annual D_{ST} minimum ($(-)D_{ST}$ maximum) values that would have been expected to occur over the last 14 solar cycles. Extreme space weather activity is often categorised in terms of D_{ST} crossing a minimum threshold. On Figure 2 we read across (green lines) *Dst* levels of $-250nT$, the threshold for 'severe' [Riley & Love, 2016] and $-500nT$, the threshold for 'great' [Lakhina & Tsu-

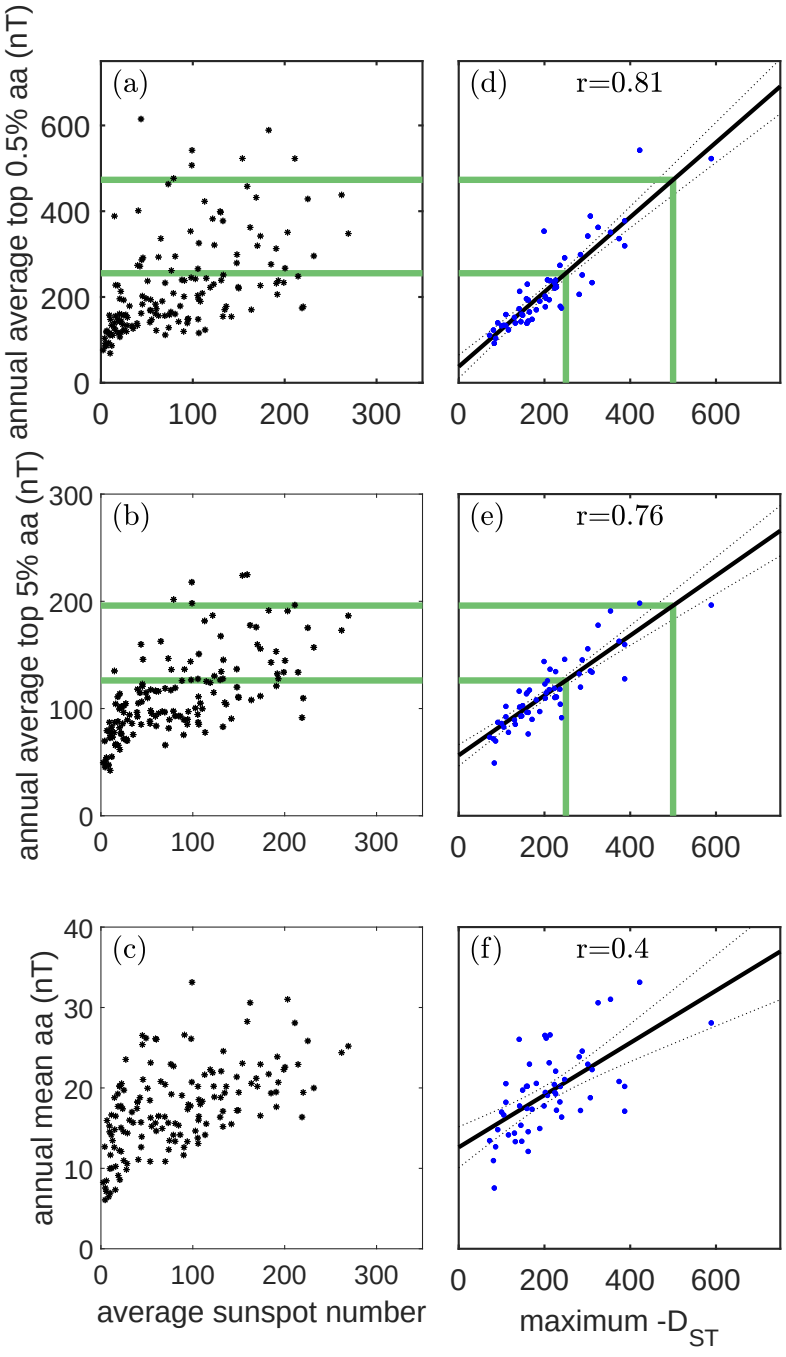

Figure 2. Panels (a-c) plot each value (black *) of the average of the largest 0.5 %, largest 5 % and all homogenized *aa* index records in each calendar year, versus average sunspot number, for all observations 1868-2017 inclusive. The annual (calendar year) intervals are non-overlapping. Panels (d-f) plot (blue dots) the subset of the non-overlapping calendar year *aa* averages versus the maximum value of $-D_{ST}$ that occurred in the same year-long window, taken over the last five solar cycles. In each panel the solid black line plots the least squares fit and the dotted lines, the 0.95 confidence level of the fit, the r-squared coefficient for each fit is given on the panels. The green lines use this fit to map between D_{ST} thresholds of $-250nT$ and $-500nT$ and corresponding *aa* values.

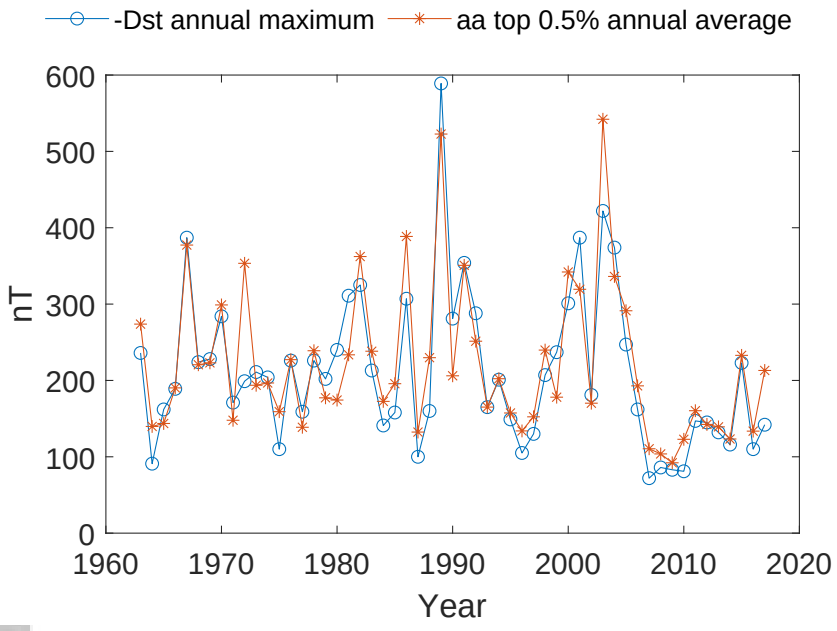

Figure 3. Comparison between $(-)D_{ST}$ and homogenized *aa* across the last 5 solar cycles. The average of the largest 0.5 % homogenized *aa* index records in each calendar year (*) is plotted alongside the maximum $(-)D_{ST}$ (o) record that occurred in that year. The calendar year samples are non-overlapping.

rutani, 2016] geomagnetic storms. *Dst* levels of $(-250, -500)$ map onto the *aa* parameters as follows: annual averages of the largest 0.5 % of the homogenized *aa*: $(255, 473)$ and annual averages of the largest 5 % of the homogenized *aa* $(126, 196)$. Counting the points that lie above these thresholds in *aa* indicates that over 150 years, on average at least one great storm occurred in 6 (4 %) of those years, and at least one severe storm occurred in 42 (28 %) of those years. These estimates average over any solar cycle variation.

We use the least squares fit in Figure 2 to read across from all 150 annual averages of the largest few % of *aa* records to the corresponding D_{ST} proxy, that is, the annual D_{ST} minimum ($(-)D_{ST}$ maximum) values that would have been expected to occur over the last 14 solar cycles. These are plotted in Figure 4 as rank order plots. In addition to the 150 annual D_{ST} proxy samples we have one additional sample that arguably exceeds all 150 values, that is, the Carrington event. The Carrington event estimate will therefore be rank 1 on this plot. The largest of the 150 annual D_{ST} proxy samples is plotted as rank 2, the next largest as rank 3 and so on.

The dependencies seen on rank order plots are simply those of the distribution [Sornette, 2003] since an empirical estimate of the cumulative density function (cdf) $C(x_k)$ is obtained by plotting rank k normalized to the total number of samples, N, $C(x_k) = k/N$ versus the samples x_k arranged in ascending order of size. The leading rank observation (rank 2 here) in 150 annual samples is then a 1/150 year event and we indicate this, and the location of a 1/10 year event across the top of the plot. To estimate the distribution functional form we have performed a least squares fit of a straight line on this semilog plot to the 100 largest ranked D_{ST} proxy samples. The green lines plot the fitted line $x_k = \beta(log(k) - b)$ where $k = [2..101]$ is the rank. The r-square values for these fits is high, $r > 0.99$. For Panel (a) of Figure 4 the fit parameters with 95% confidence in brackets are $\beta = -146$ $[-148, -144]$ and $b = 5.53$ $[5.50, 5.56]$. The high r-square value of these fitted lines confirms that the tail of the distribution is well described by an exponential function [Sornette, 2003] $f(x) = (1/\beta)exp(-x/\beta)$. The 95% confidence intervals

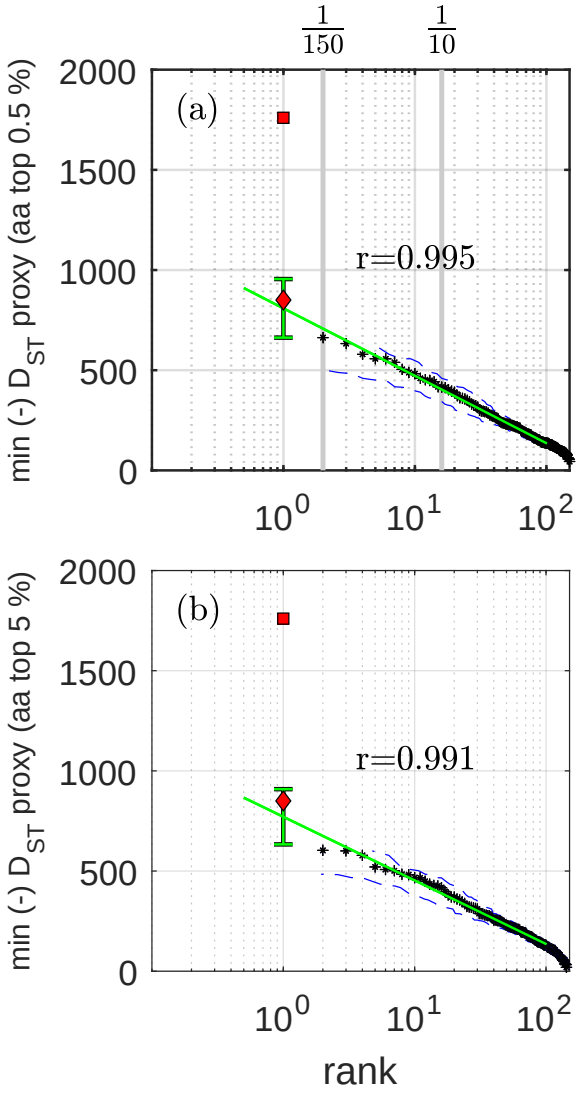

Figure 4. The panels show rank order plots of non-overlapping annual minimum $(-)D_{ST}$ proxy samples derived from: (a) the largest 0.5 % and (b) the largest 5 % of homogenized *aa* (black stars). The largest of these samples is plotted as rank 2, the next largest as rank 3 and so on. We plot as rank 1 two estimates of the Carrington event: $D_{ST} = -850nT$ (red diamond) and $D_{ST} = -1760nT$ (red square). The green lines indicates an exponential fit to the largest 100 values and the r-squared coefficient for each fit is given in the panels. The error bars for the the first ranked sample (green error bar) are estimated for an underlying exponential distribution (see text). The 95% confidence level for this empirical realization of the rank order plot are estimated from *Greenwood* [1926] (blue dashed lines).

Top ten most active years in the *aa* index record

rank	year	% chance per year	activity in that year
1	1921	0.67 [0, 1.9]	Remarkable storm[1]; Silverman & Cliver [2001], Table IV, VII[2]
2	1938	1.33 [0, 3.1]	Fátima storm; Table III,IV,VII[2]
3	2003	2.0 [0, 4.2]	Halloween storms; Weaver [2004], Table III[2]
4	1946	2.67 [0.1, 5.2]	Table IV[2]
5	1989	3.33 [0.5, 6.3]	Quebec power outage[1]; MacNeil [2018]; Table VII[2]
6	1882	4.0 [0.9, 7.1]	Remarkable storm[1]; Love [2018], Table IV[2]
7	1941	4.67 [1.3, 8.1]	geomagnetic storm; Love & Coïsson [2016];Table III,IV[2]
8	1909	5.33 [1.7, 8.9]	Remarkable storm[1];Love et al. [2019a] Table IV, VII[2]
9	1960	6.0 [2.2, 9.8]	Table III[2]
10	1958	6.67 [2.7, 10.7]	Remarkable storm[1]; Table VII[2]

Table 1. Rank ordering of the most active years with chance of occurrence from Figure 4. Remarkable storms[1](geomagnetic perturbation, Table 1 of Tsurutani et al. [2003]). Events[2] in Cliver & Svalgaard [2004] Tables III (fast transit events up to 2003), IV (Greenwich list of great storms up to 1954), VII (low latitude auroras up to 1958).

for this fitted line give an uncertainty that deviates less than 1% from the fitted line. The dominant uncertainty on this plot arises from the variation between different empirical realisations of the cdf (or rank order plot) for which *Greenwood* [1926] provides an estimate as shown on the Figure. Applying this uncertainty to the results from Figure 4 then gives the chance of at least one great $D_{ST} < -500nT$ storm in a given year is then 4% with uncertainty bounds [0.9,7], and for a severe, $D_{ST} < -250nT$ storm is 28% [20,35]. The top ten most active years in the 150 year *aa* record (plotted as rank $k = 2..11$ on Figure 4) are summarised in Table 1. As we would expect, years in which some of the most severe storms occurred appear here, however we can now directly rank them and can estimate their % occurrence likelihood.

An important question is whether the Carrington event belongs to the same physical class as the other super-storms. If so, its probable severity and chance of occurrence should be predictable at least in principle, as it will follow that of the other more moderate super-storms. If not, it is in a distinct physical class and past observations of more moderate super-storms may not inform estimates of its chance of occurrence; it is a 'Dragon King' [Sornette & Ouillon, 2012]. We now determine if estimates for the Carrington event are consistent with the exponential distribution of proxy D_{ST}. For an exponential we have [Sornette, 2003] an estimate of the fluctuations between one realization to another for the first ranked sample, it is $\pm\beta$. This is plotted as a green error bar on the rank 1 location of the exponential fit. This gives an estimate $D_{ST} = -809$ $[-663, -955]$ (using classic *aa* as shown in the SI we obtain $D_{ST} = -813$ $[-667, -959]$). This is the range of values for D_{ST} for this event to be a 1 in 151 year event drawn from the same distribution as other extreme activity seen in *aa* over the last 14 solar cycles. We overplot at rank 1 the two estimates of the Carrington event (red diamond and square). From Figure 4 we see that the estimate of $D_{ST} = -850nT$ is consistent with the above extrapolation of the exponential fit so that the likelihood of any given year exhibiting a Carrington-class event on this scale simply follows the exponential distribution that describes the other severe storms that have occurred since. However, a value of of $D_{ST} = -1760nT$ (red square) is in its own class of behaviour, it is far from this exponential distribution tail.

The D_{ST} excursion that occurred during historical space weather events is challenging to quantify, and as a consequence, there is considerable diversity in both the values

obtained and the methodology used to obtain them. The $D_{ST} = -1760nT$ estimate for the Carrington event is a minimum magnetic displacement in a Bombay magnetogram[Tsurutani et al., 2003] and Lakhina & Tsurutani [2016] discuss supporting evidence that this is indeed consistent with this D_{ST} value. The Bombay station was fortuitously located near noon during the peak magnetometer displacement so that the effect of the disturbance field asymmetry is minimised, and local H component values are close to D_{ST} (see eg Figure 2 of Siscoe et al. [2006]). However, given that D_{ST} is an hourly index, this value has has been interpreted by Siscoe et al. [2006] (see also Cliver & Dietrich [2013]) as a minimum $D_{ST} \approx -850nT$ based on hourly averages of the Bombay magnetogram. Different versions [Tsurutani et al., 2003; Siscoe et al., 2006] of the Burton et al. [1975] equation support these two different estimates. Other observations offer insight; Hayakawa et al. [2019] found that the equatorward boundary of auroral oval of the Carrington event was comparable with that of other super-storms, suggesting a D_{ST} value closer to that of Siscoe et al. [2006]. Modelling of the 'solar storm' of 2012, an intense CME which did not impact on earth but was observed at STEREO-A, suggest extreme case scenarios of $D_{ST} = -1182nT$ [Baker et al., 2013] and $D_{ST} = -1150nT$ [Liu et al., 2012]. In the 2012 solar storm, the correlated dynamics of several CMEs created the conditions for an unusually intense event. The analysis in this Letter does not rule out any of these estimates. Instead, it offers quantitative insight into their interpretation. Events with $D_{ST} \lesssim -1000nT$ are a different class of behaviour to other severe storms that have occurred over the last 150 years. They require special conditions which may be physical, observational, or a combination thereof.

We have parameterized extreme space weather activity with annual averages of the top few % of the *aa* index. Whilst this has allowed us to form a distribution from observations over 14 solar cycles, it does not discriminate the statistics of individual events. This can only be done for time-series that are well resolved in amplitude, such as D_{ST}, for which there are a number of studies. We have identified a correspondence between the annual averages of the top few % of the *aa* index and the annual minimum D_{ST}, that is, the largest event in each year. In general, for moderate conditions, there will be several storms per year, so that the return period of a level of annual activity that we find here would not be expected to correspond to the return period for an event of a specific amplitude. For the most severe and infrequent storms there will be closer correspondence between these two measures. Our estimate that a $D_{ST} \sim -850nT$ is a ~ 1 in 150 year event is not inconsistent with that of Riley & Love [2016], a 10% [1,20] chance of occurrence per decade. The D_{ST} excursion $907 \pm 132nT$ Love et al. [2019b] estimate for the 1921 event also overlaps with the range determined here for the rank 1 event. Tsubouchi & Omura [2007] predicts an occurrence frequency of a March 1989 storm intensity ($D_{ST} = -589nT$) or greater as once in 60 years. In Figure 4, 1989 is ranked the 5th most active year in 150 years of *aa* observations, giving a return period of 30 years.

5 Conclusions

The *aa* index extends over the last 14 solar cycles, it is the longest almost continuous record of geomagnetic activity at the earth's surface. However the *aa* index is constructed from observations that are logarithmically discretized in amplitude and thus individual records of the 3 hour *aa* index will have uncertainties that are both significant and non-trivial to estimate [Bubenik & Fraser-Smith, 1977]; in particular its extreme excursions are not well resolved in amplitude. We parameterized extreme *aa* activity using averages of the annual top few % of observed records. Our analysis based on rank order plots [Sornette, 2003] shows that the distribution tail (of the top 100 annual estimates of extreme *aa* activity) is well described by an exponential distribution ($r > 0.99$). The D_{ST} index is available for the last five solar cycles and as its amplitude is well resolved it is commonly used to characterise the intensity of space weather events. We found a good correspondence ($r \sim 0.8$) between the annual minimum D_{ST} value and the annual aver-

aged top few (0.5 %, 5%) values of aa over the last five solar cycles. This can be used to 'read across' between annual minimum D_{ST} values and extreme activity in aa.

We then find that least one 'severe' storm of $D_{ST} < -250nT$ occurred in each of 42 (~28% [20,35]) of those years and at least one 'great' storm $D_{ST} < -500nT$ occurred in each of 6 (~4% [0.9,7]) of those years. These estimates are an overall average and do not take into account any solar cycle phase variation. By sampling over 14 solar cycles, they do include a greater variety of solar cycle intensities than estimates that rely upon data from the last five cycles.

We extended this analysis to D_{ST} estimates for the Carrington event, to compare them with the annual level of extreme activity seen in aa. Extrapolating our exponential distribution gives an estimate $D_{ST} = -809$ $[-663, -955]$ for a 1 in 151 year event that follows the same distribution as other extreme activity seen in aa over the last 14 solar cycles. The occurrence of a $D_{ST} \sim -850nT$ [Siscoe et al., 2006] event in a single year is consistent with this distribution tail. A Carrington event on this scale is a more intense version of the other super-storms that have occurred since 1868, so that in this case the set of observed super-storms can be used to predict how likely such an event is in the future. A $D_{ST} \sim -1760nT$ Carrington event on the other hand is far from the distribution tail and is in a class of its own, it is a 'Dragon King' [Sornette & Ouillon, 2012] requiring the concurrence of special conditions in the corona and solar wind and at the earth. The 2012 "solar storm" [Liu et al., 2012] is an event in this class, where the correlated dynamics of several CMEs created the conditions for an unusually intense event.

Acknowledgments

The results presented in this paper rely in part on geomagnetic indices calculated and made available by ISGI Collaborating Institutes from data collected at magnetic observatories. We acknowledge the involved national institutes, the INTERMAGNET network and ISGI (isgi.unistra.fr). We also acknowledge Lockwood et al. [2018b,c] for the provision of the homogenous aa index used here. We thank the World Data Center for Geomagnetism, Kyoto. We thank the World Data Center SILSO, Royal Observatory of Belgium, Brussels for provision of sunspot data.

SCC acknowledges a Fulbright-Lloyd's of London Scholarship and AFOSR grant FA9550-17-1-0054 and ST/P000320/1. RBH acknowledges the NERC Highlight topic grant NE/P01738X/1 (Rad-Sat) and NE/R016038/1.

Data availability: The ISGI aa index dataset analysed here was downloaded from the International Service of Geomagnetic Indices at http://isgi.unistra.fr/. The homogenized aa index analysed here was downloaded from the SI of Lockwood et al. [2018c] at https://www.swsc-journal.org/articles/swsc/olm/2018/01/swsc180022/swsc180022.html. The daily sunspot number dataset was downloaded from the SILSO, World Data Center - Sunspot Number and Long-term Solar Observations, Royal Observatory of Belgium, online Sunspot Number catalogue: http://www.sidc.be/SILSO/, '1868-2017' The D_{ST} index analysed here was downloaded from NASA/GSFC's Space Physics Data Facility's OMNIWeb service, the OMNI data were obtained from the GSFC/SPDF OMNIWeb interface at https://omniweb.gsfc.nasa.gov.

References

Baker, D. N., X. Li, A. Pulkkinen, C. M. Ngwira, M. L. Mays, A. B. Galvin, K. D. C. Simunac, (2013) A major solar eruptive event in July 2012: Defining extreme space weather scenarios, Space Weather, 11, 585, DOI:10.1002/swe.20097

Baker, D. N., & Lanzerotti, L. J. (2016). Resource Letter SW1: Space weather, Am. J. Phys. 84, 166. DOI:10.1119/1.4938403

Bartels, J., Heck, N. H., Johnston, H. F. (1939) The three-hour-range index measuring geomagnetic activity, J. Geophys. Res., DOI:10.1029/TE044i004p00411

Bubenik, D. M., Fraser-Smith, A. C., (1977) Evidence for strong artificial components in the equivalent linear amplitude geomagnetic indices, J. Geophys. Res., 82, 2875

Burton, R.K., McPherron, R.L., Russell, C.T.(1975) An empirical relationship between interplanetary conditions and Dst. J. Geophys. Res. 80, 4204

Cannon, P., Angling M., Barclay, L., Curry, C., Dyer, C., Edwards, R., Greene, G., Hapgood, M., Horne, R. B., Jackson, D., Mitchell, C. N., Owen, J., Richards, A., Rodgers, C., Ryden, K., Saunders, S., Sweeting, M., Tanner, R., Thomson, A. and Underwood, C., (2013) Extreme Space Weather: Impacts on Engineered Systems and Infrastructure, pp. 1-68, Royal Academy of Engineering, London, United Kingdom.

Chapman, S. C., Watkins, N. W., Tindale, E., (2018) Reproducible aspects of the climate of space weather over the last five solar cycles, Space Weather, DOI:10.1029/2018SW001884

Cliver, E. W., Svalgaard, L., (2004) The 1859 solar-terrestrial disturbance and the current limits of extreme space weather activity, Solar Physics, 224: 407-422

Cliver, E. W., W. F. Dietrich, (2013) The 1859 space weather event revisited: limits of extreme activity, J. Space Weather Space Clim. 3, 31, DOI: 10.1051/swsc/2013053

Daglis, I. A. (ed.) (2004) Effects of space weather on technology infrastructure, pp. 1-334, Kluwer Academic Publishers, Dordrecht, The Netherlands.

Elvidge, S., Angling, M. J. (2018). Using Extreme Value Theory for Determining the Probability of Carrington-Like Solar Flares. DOI:10.1002/2017SW001727

Feynman, J., (1982). Geomagnetic and solar wind cycles, 1900-1975, J. Geophys. Res., 87(A8), 6153 DOI:10.1029/JA087iA08p06153

Greenwood, M. (1926). The Natural Duration of Cancer, in Reports of Public Health and Related Subjects, Vol. 33, HMSO, London.

Hathaway, D. H. (2015) The solar cycle, Living Rev. Solar Phys., 12, 4. DOI:10.1007/lrsp-2015-4

Hayakawa H., et al. (2019) Temporal and Spatial Evolutions of a Large Sunspot Group and Great Auroral Storms around the Carrington Event in 1859, Space Weather DOI: 10.1029/2019SW002269

Hush, P., S. C. Chapman, M. W. Dunlop, N. W. Watkins (2015), Robust statistical properties of the size of large burst events in AE, Geophys. Res. Lett., 42, DOI:10.1002/2015GL066277.

Kelly, G. S., Viljanen, A., Beggan, C. D., Thomson, A. W. P., (2016) Understanding GIC in the UK and French high-voltage transmission systems during severe magnetic storms, Space Weather, 15, 99-114, DOI:10.1002/2016SW001469

Lakhina G. S., Tsurutani B. T. (2016). Geomagnetic storms: historical perspective to modern view. Geosci. Lett. 3:5 DOI:10.1186/s40562-016-0037-4

Liu, Y. D., Luhmann, J. G., Kajdic, P., E.,Kilpua, K. J., Lugaz, N., Nitta, N. V.,östl, C. M., Lavraud, B., Bale, S. D., Farrugia, C. J., Galvin, A. B., (2014) Observations of an extreme storm in interplanetary space caused by successive coronal mass ejections, Nat. Com. 5, 3481 DOI:10.1038/ncomms4481

Lockwood, M., Owens, M. J., Barnard, L. A., Scott, C. J., Watt, C. E., Bentley, S., (2018a). Space climate and space weather over the past 400 years: 2. Proxy indicators of geomagnetic storm and substorm occurrence, J. Space Weather Space Climate, 8, A12. DOI:10.1051/swsc/

Lockwood, M., A. Chambodut, L.A. Barnard, M.J. Owens, and E. Clarke (2018b) A homogeneous aa index: 1. Secular variation, J. Space Weather Space Climate, DOI:10.1051/swsc/2018038

Lockwood, M., I.D. Finch, A. Chambodut, L.A. Barnard, M.J. Owens, and E. Clarke (2018c) A homogeneous aa index: 2. hemispheric asymmetries and the equinoctial variation, J. Space Weather Space Climate

Love, J. J., Rigler, E. J., Pulkkinen, A. and Riley, P., (2015). On the lognormality of historical magnetic storm intensity statistics: Implications for extreme-event probabilities, Geophys. Res. Lett., 42(16), 6544-6553, DOI:10.1002/2015GL064842

Love, J. J., (2018) The Electric Storm of November 1882. Space Weather, 16, DOI:10.1002/2017SW001795.

Love, J. J., Coïsson, P., (2016) The Geomagnetic Blitz of September 1941, Eos. 97. doi:10.1029/2016EO059319.

Love, J. J., Hayakawa, H., & Cliver, E. W. (2019). On the intensity of the magnetic superstorm of September 1909. Space Weather, 17, 37-45. DOI:10.1029/2018SW002079

Love, J. J., Hayakawa, H., Cliver, E. W. (2019). Intensity and impact of the New York Railroad superstorm of May 1921. Space Weather, 17, 1281–1292. DOI: 10.1029/2019SW002250

MacNeil, J. (2018) Solar explosion leads to blackout, March 10, 1989. EDN Network, March 10

Mayaud, P-N. (1972) The aa indices: A 100 year series characterizing the magnetic activity, J. Geophys. Res., 77, 6870

Mayaud, P. N. (1980). Derivation, Meaning, and Use of Geomagnetic Indices, Geophys. Monogr. Ser., vol. 22, AGU, Washington, D.C. DOI:10.1029/GM022

Oughton, E. J., A. Skelton, R. B. Horne, A. W. P. Thomson, and C. T. Gaunt (2017), Quantifying the daily economic impact of extreme space weather due to failure in electricity transmission infrastructure, Space Weather, 15, DOI:10.1002/2016SW001491.

Riley, P. (2012). On the probability of occurrence of extreme space weather events, Space Weather 10, S02012.

Riley, P., Love, J. J., (2016) Extreme geomagnetic storms: Probabilistic forecasts and their uncertainties, Space Weather, 15, 53-64, DOI:10.1002/2016SW001470.

Silverman S. M. and Cliver E. W., (2001) Low-latitude auroras: the magnetic storm of 14-15 May 1921. Journal of Atmospheric and Solar Terrestrial Physics, 63(5):523-535.

Silbergleit, V. M. (1996). On the occurrence of geomagnetic storms with sudden commencements, J. Geomagn. Geoelectr., 48, 1011.

Silbergleit, V. M. (1999). Forecast of the most geomagnetically disturbed days, Earth Planets Space, 51, 19. DOI:10.1186/BF03352205

Siscoe, G. L. (1976). On the statistics of the largest geomagnetic storms per solar cycle, J. Geophys. Res., 81, 4782. DOI:10.1029/JA081i025p04782

G. Siscoe, N. U. Crooker, C. R. Clauer, (2006) D_{st} of the Carrington storm of 1859, Adv. Space. Res. 38, 173-179

Sornette, D. (2003) Critical phenomena in natural sciences, 2nd Ed. Springer

Sornette, D., Ouillon, G., (2012) Dragon-kings: mechanisms, statistical methods and empirical evidence. The European Physical Journal Special Topics 205.1 1-26

Sugiura, M., (1964) Hourly value of equatorial Dst for the IGY, Ann. Int. Geophys. Year, 35, 9-45.

Sugiura, M. & Kamei, T., (1991) Equatorial Dst index 1957-1986, IAGA Bull., 40, ISGI Publication Office, Saint-Maur-des-Fossess, France.

Thomson, A. W. P., Gaunt, C. T., Cilliers, P., Wild, J. A., Opperman, B., McKinnell, L.-A., Kotze, P., Ngwira, C.M., Lotz, S.I., Present day challenges in understanding the geomagnetic hazard to national power grids (2010) Adv. Space Res. 45 1182-1190 DOI:10.1016/j.asr.2009.11.023

Thomson, A. W. P, Dawson, E. B., Reay, S. J. (2011). Quantifying extreme behaviour in geomagnetic activity, Space Weather, 9, S10001. DOI:10:1029/2011SW000696

Tindale, E., S. C. Chapman (2016), Solar cycle variation of the statistical distribution of the solar wind ϵ parameter and its constituent variables, Geophys. Res. Lett., 43, DOI:10.1002/2016GL068920.

Tindale, E., Chapman, S. C. (2017). Solar wind plasma parameter variability across solar cycles 23 and 24: From turbulence to extremes. Journal of Geophysical Research: Space Physics, 122. DOI:10.1002/2017JA024412

Tsubouchi, K., Omura, Y. (2007). Long-term occurrence probabilities of intense geomagnetic storm events, Space Weather, 5, S12003. DOI:10.1029/2007SW000329

Tsurutani, B. T., Gonzalez, W. D., Lakhina, G. S., Alex, S., (2003) The extreme magnetic storm of 1-2 September 1859, J. Geophys. Res., 108(A7), 1268, DOI:10.1029/2002JA009504

Tsurutani, B. T., et al. (2006) Corotating solar wind streams and recurrent geomagnetic activity: A review, J. Geophys. Res., 111, A07S01, DOI:10.1029/2005JA011273.

Weaver, M., Murtagh, W., et al. (2004) Halloween Space Weather Storms of 2003, NOAA Technical Memorandum. OAR SEC-88. Boulder, CO: Space Environment Center. OCLC 68692085

World Data Center for Geomagnetism, Kyoto, M. Nose, T. Iyemori, M. Sugiura, T. Kamei (2015), Geomagnetic Dst index, DOI:10.17593/14515-74000.

Figure 1.

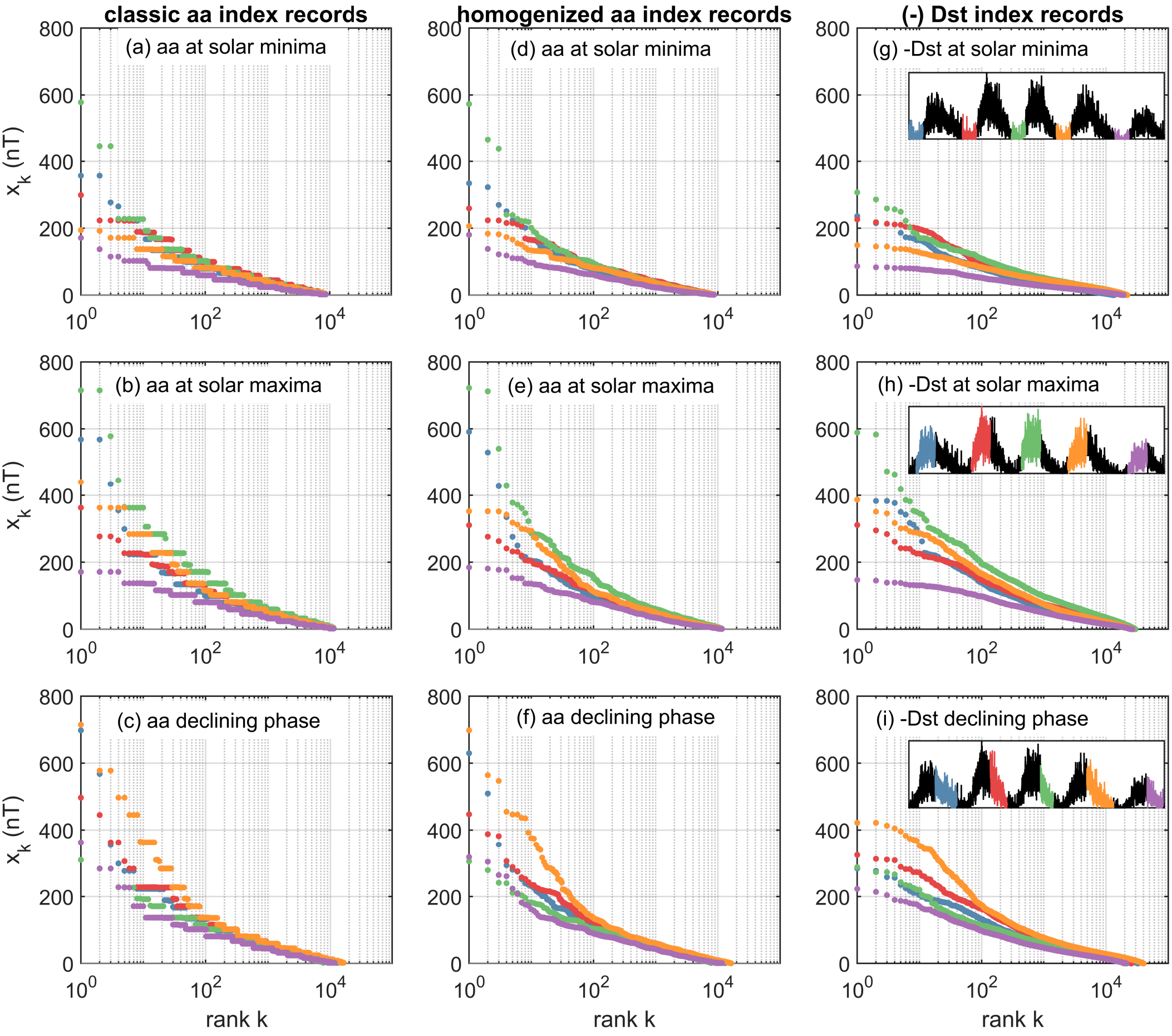
classic aa index records
homogenized aa index records
(-) Dst index records
(a) aa at solar minima
(b) aa at solar maxima
(c) aa declining phase
(d) aa at solar minima
(e) aa at solar maxima
(f) aa declining phase
(g) -Dst at solar minima
(h) -Dst at solar maxima
(i) -Dst declining phase
x_k (nT)
rank k
800
600
400
200
0
10^0
10^2
10^4

Figure 2.

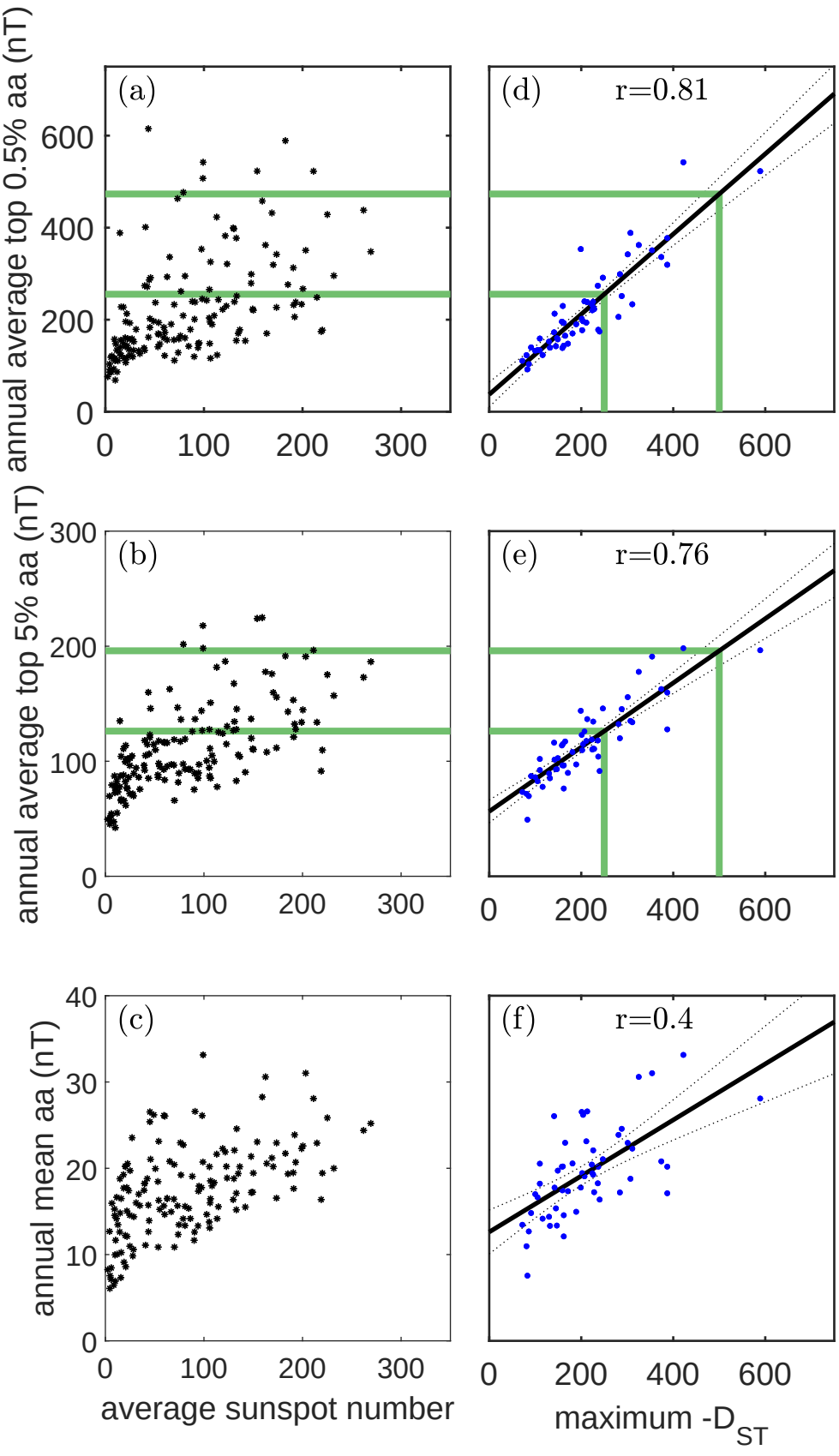
(a)
(b)
(c)
(d)
r=0.81
(e)
r=0.76
(f)
r=0.4
annual average top 0.5% aa (nT)
annual average top 5% aa (nT)
annual mean aa (nT)
average sunspot number
maximum -D$_{ST}$
0
100
200
300
400
600

Figure 3.

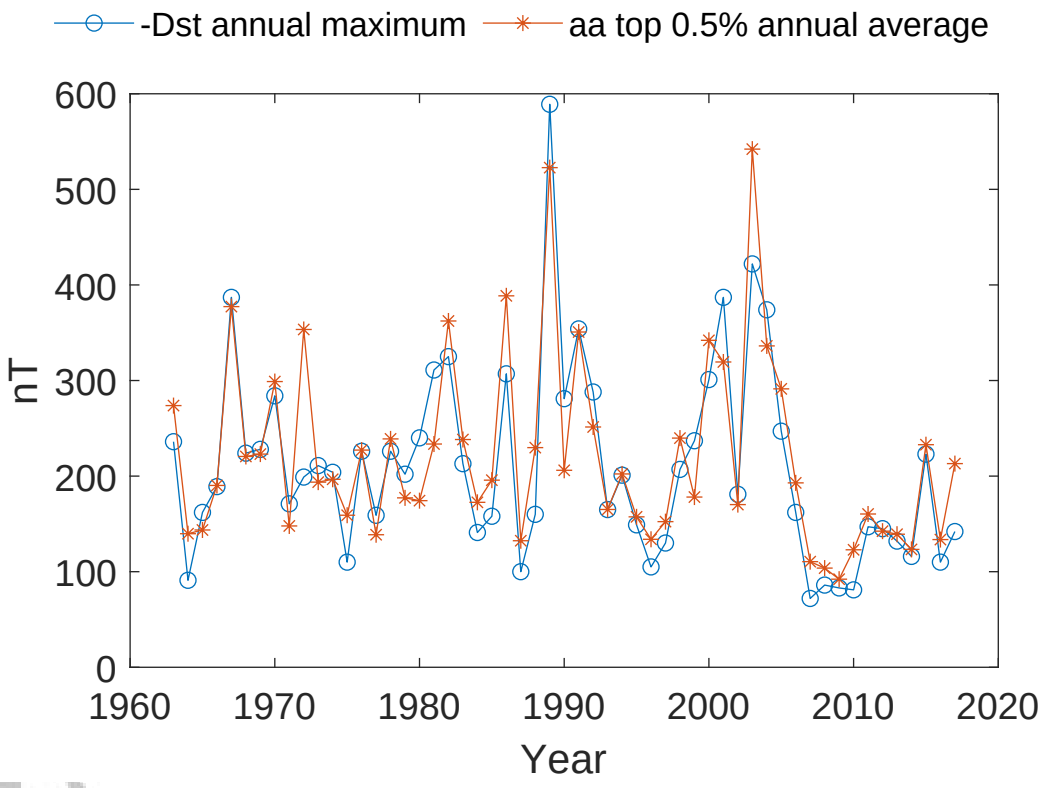

Figure 4.

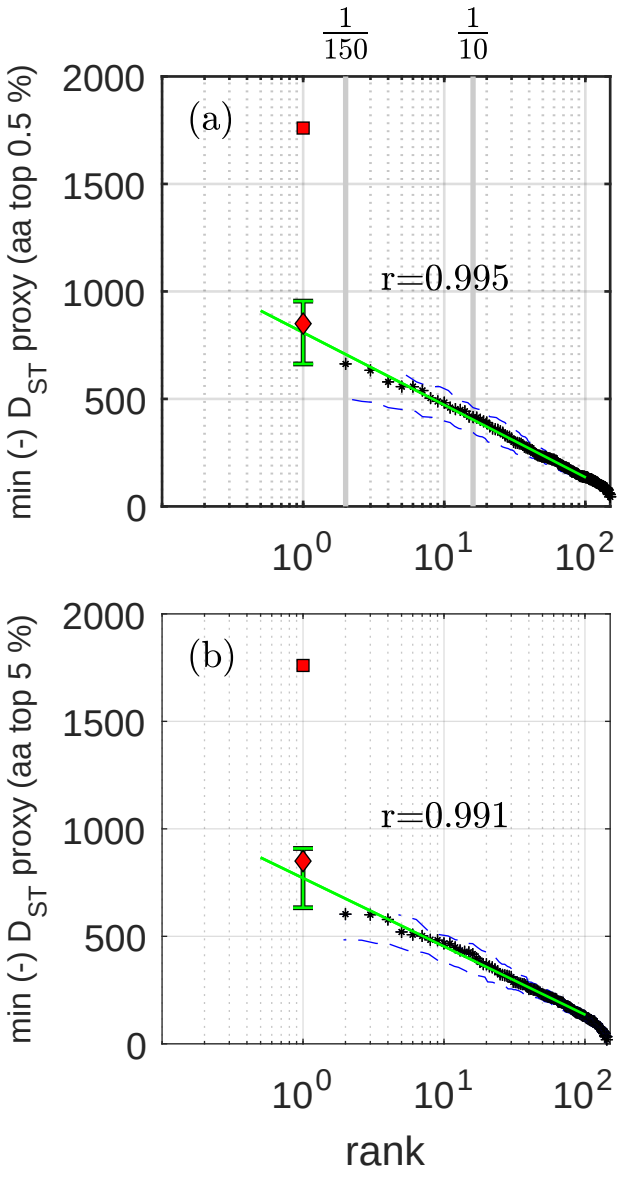
1/150
1/10
(a)
r=0.995
min (-) D_ST proxy (aa top 0.5 %)
2000
1500
1000
500
0
10^0
10^1
10^2
(b)
r=0.991
min (-) D_ST proxy (aa top 5 %)
rank

Supporting Information for "Using the *aa* index over the last 14 solar cycles to characterize extreme geomagnetic activity."

S. C. Chapman[1], R. B. Horne[2], and N. W. Watkins[1,3,4]

[1]Centre for Fusion, Space And Astrophysics, Physics Department, University of Warwick, Coventry CV4 7AL
[2]British Antarctic Survey, Cambridge, CB3 0ET, UK
[3]Centre for the Analysis of Time Series, London School of Economics and Political Science, London, WC2A 2AZ, UK
[4]School of Science, Technology, Engineering and Mathematics, The Open University, Milton Keynes, UK

Contents

1. Figure 1 plots the *aa* index and daily sunspot number over the last 14 solar cycles.
2. Figures 2 and 3 show the intervals selected for the minima, maxima and declining solar cycle phases. Each solar cycle is of a different duration. We take the minima identified from the quietest days of the solar cycle 13-month mean of the International Sunspot Number and then identify intervals for the maximum, declining phase and minimum phase by applying a simple algorithm across the entire dataset. The maximum phase begins 1.5 years after the previous sunspot quietest day minimum and lasts for 4 years at which the declining phase begins. The minimum phase is of 3 years duration centred on the sunspot quietest day minimum.
3. In the main text we used the homogenized *aa* index; the remaining Figures reproduce key Figures using the classic *aa* index.

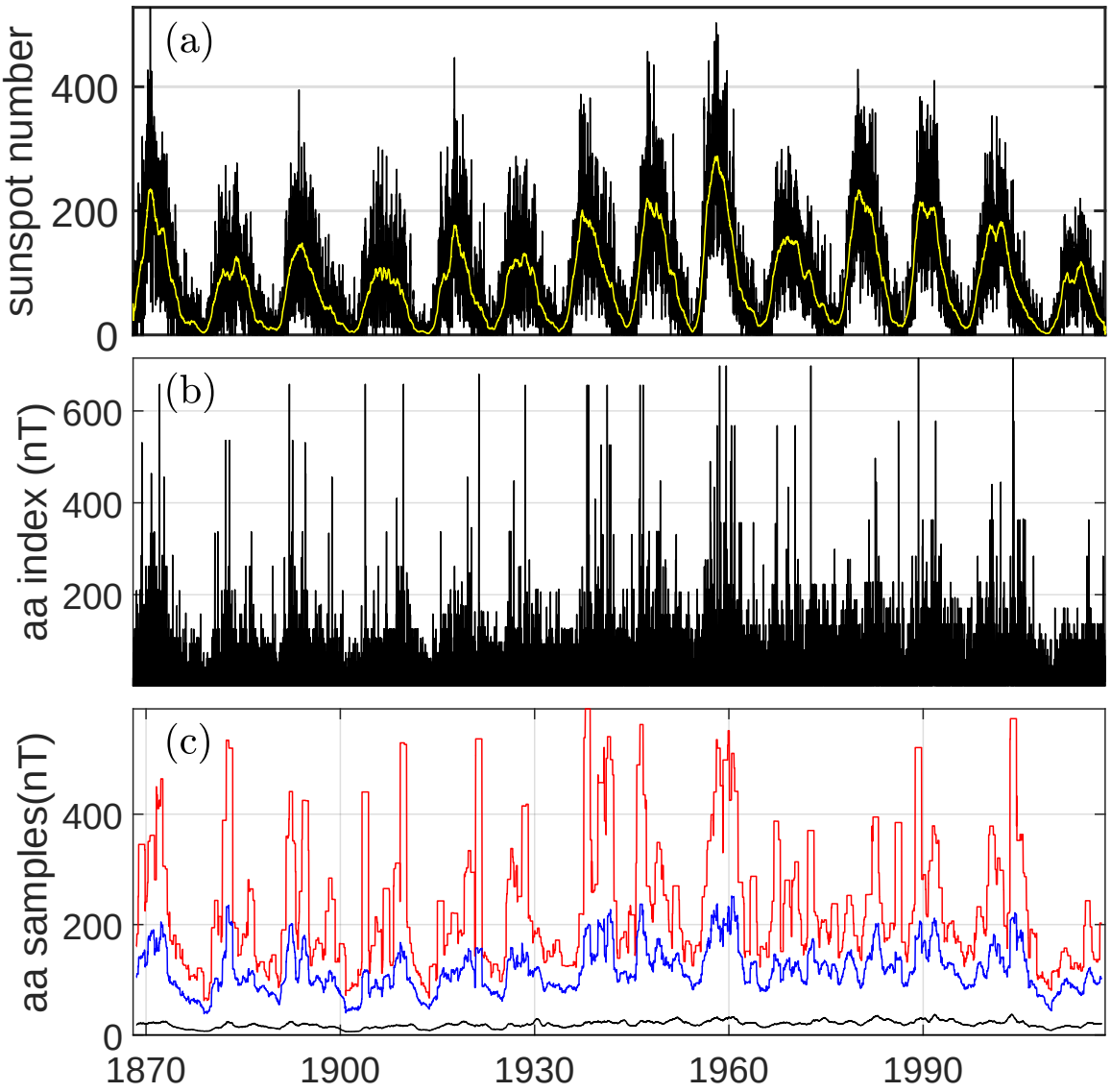

Figure 1. The *aa* index and daily sunspot number over the last 14 solar cycles. From top to bottom the panels plot: (a) the daily sunspot number, with a 1 year running average in yellow; (b) records of the classic 3-hour *aa* index; and (c) a 1 year running sample average of the largest 0.5% (red), largest 5% (blue) and all values (black) of the *aa* index.

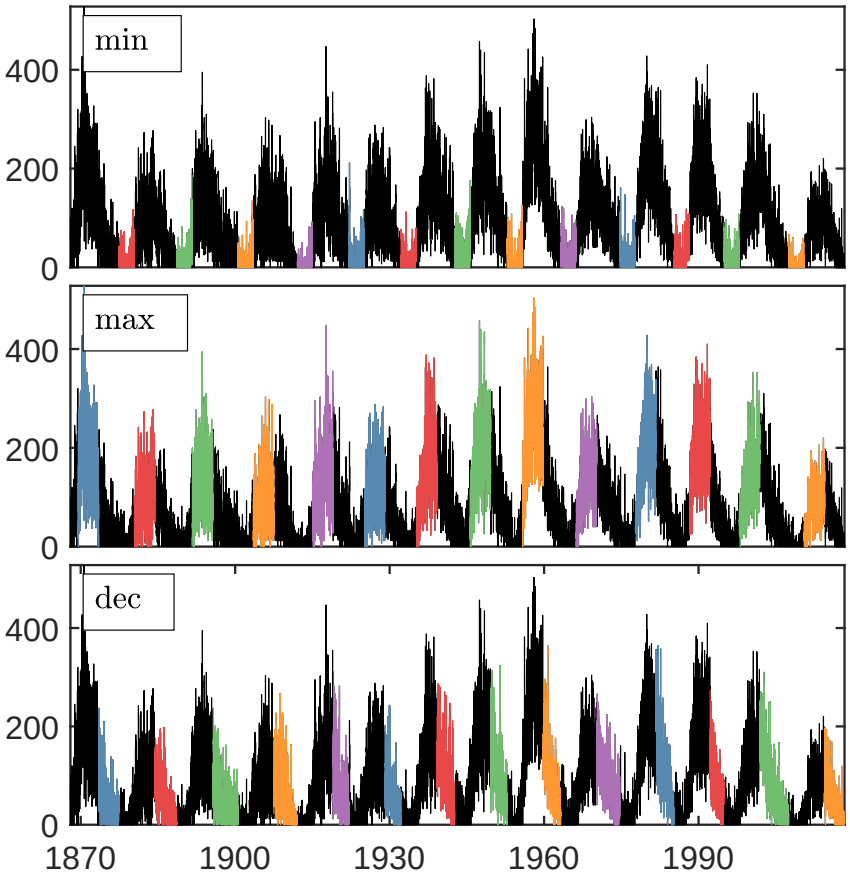

Figure 2. The panels plot from top to bottom: daily sunspot number time-series overplotted to show the intervals selected for the minima, maxima and declining solar cycle phases.

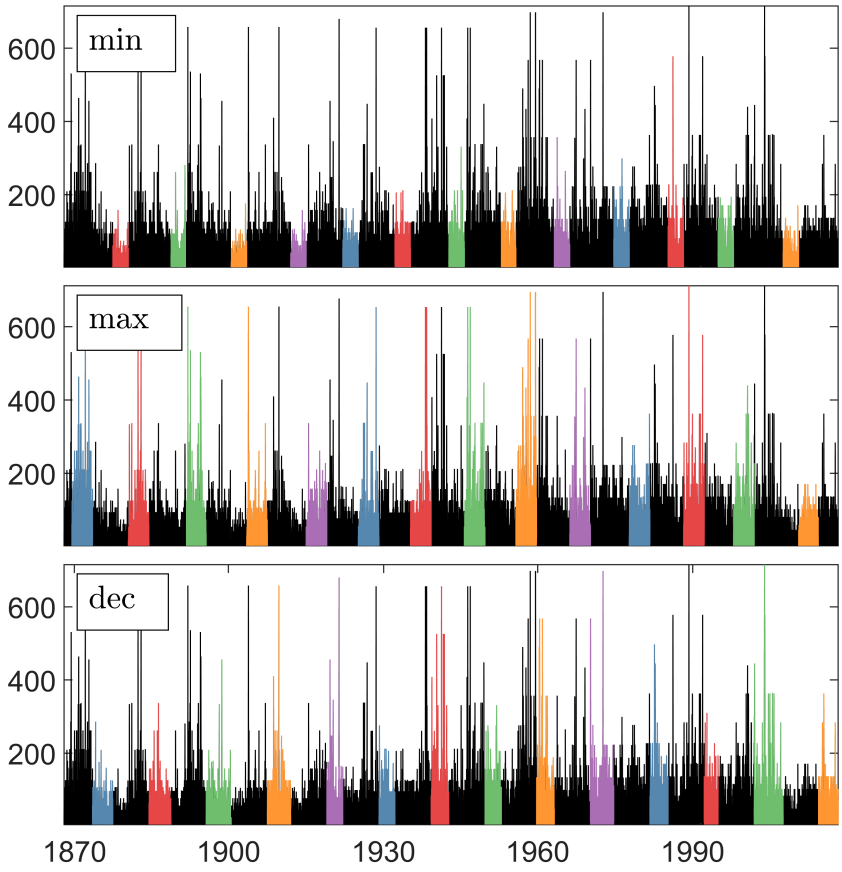

Figure 3. The panels plot from top to bottom: the 3 hourly classic *aa* index time-series overplotted to show the intervals selected for the minima, maxima and declining solar cycle phases.

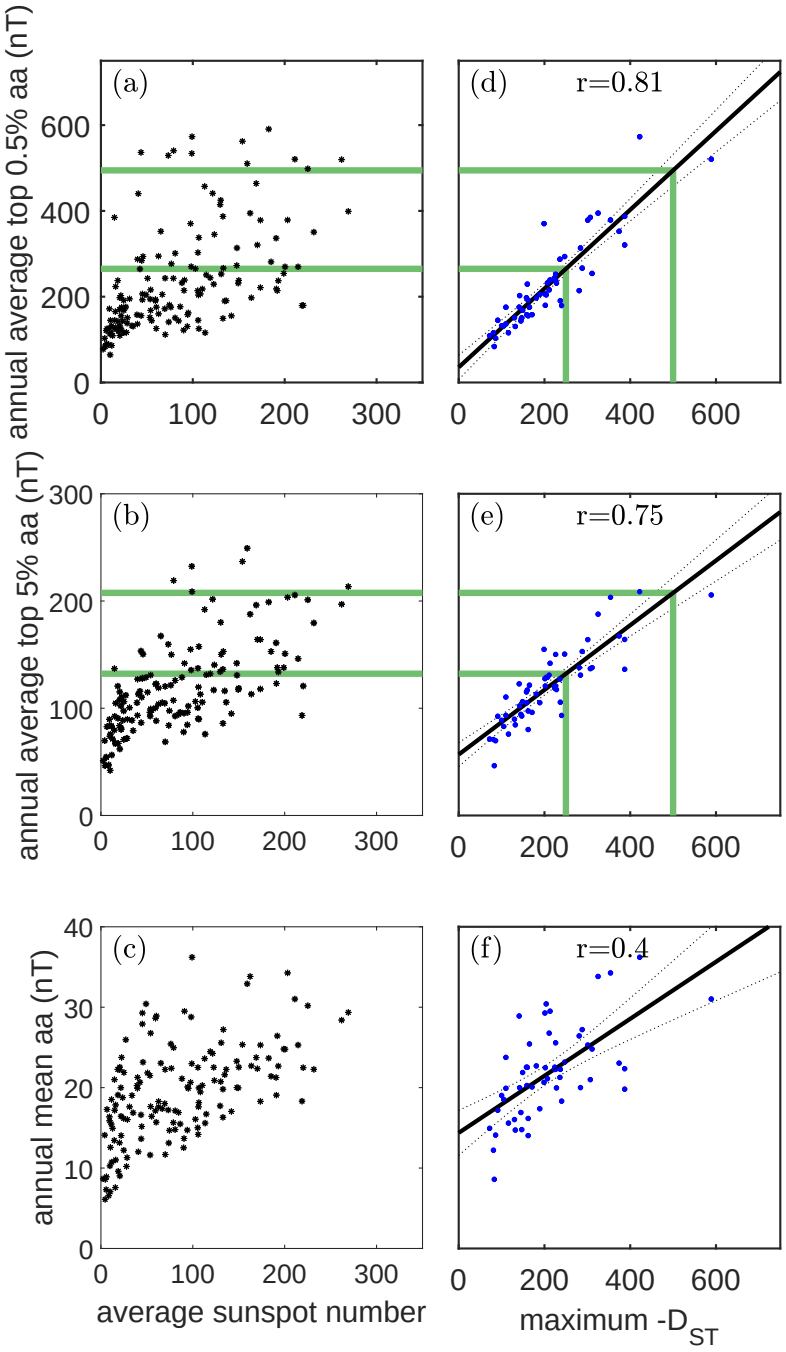

Figure 4. Panels (a-c) plot each value (black *) of the average of the largest 0.5 %, largest 5 % and all classic *aa* index records in each calendar year, versus average sunspot number, for all observations 1868-2017 inclusive. The annual (calendar year) intervals are non-overlapping. Panels (d-f) plot (blue dots) the subset of the non-overlapping calendar year *aa* averages versus the maximum value of $-D_{ST}$ that occurred in the same year-long window, taken over the last five solar cycles. In each panel the solid black line plots the least squares fit and the dotted lines, the 0.95 confidence level of the fit. The green lines use this fit to map across D_{ST} thresholds of $-250nT$ and $-500nT$ to corresponding *aa* values.

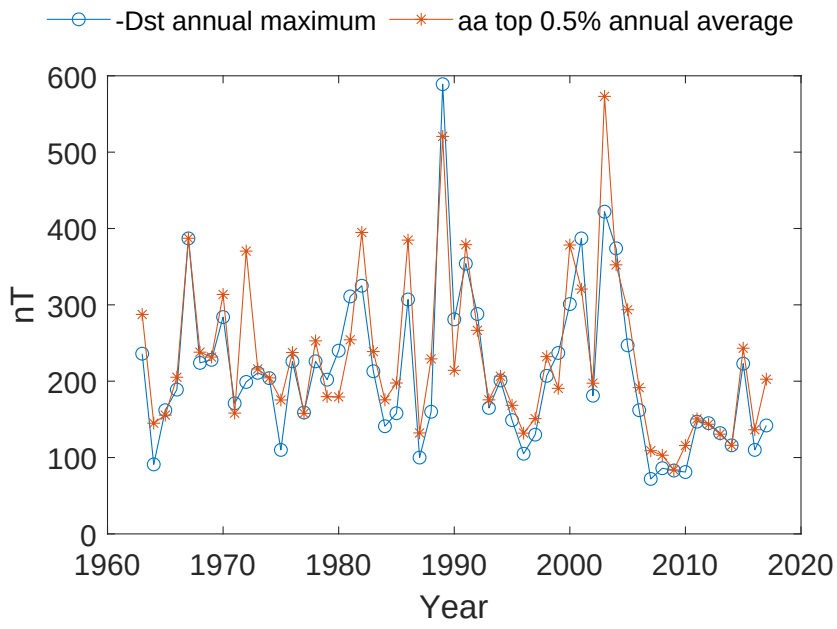

Figure 5. Comparison between $(-)D_{ST}$ and classic *aa* across the last 5 solar cycles. The average of the largest 0.5 % classic *aa* index records in each calendar year (*) is plotted alongside the maximum $(-)D_{ST}$ (o) record that occurred in that year. The calendar year samples are non-overlapping.

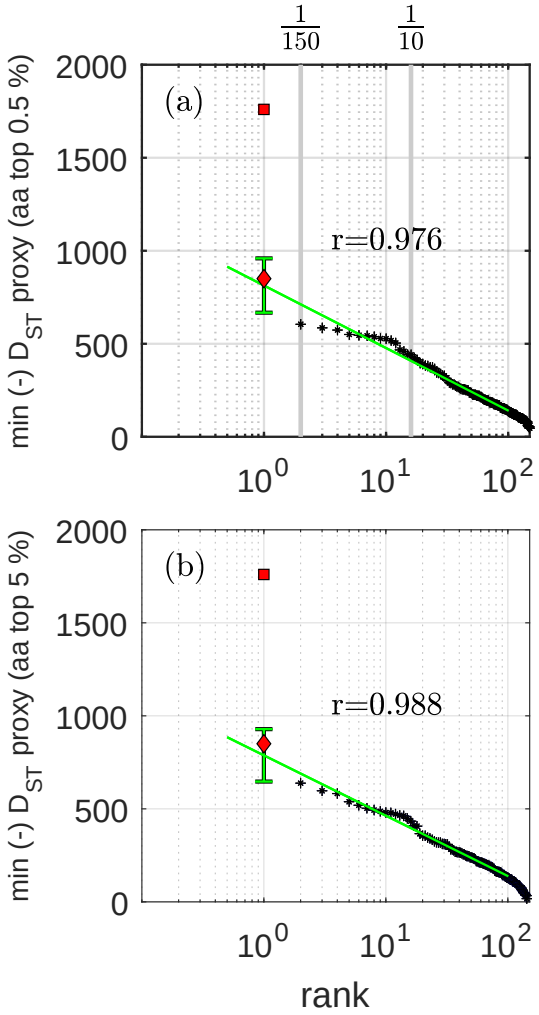

Figure 6. Rank order plots of parametrized classic *aa* shown in Figure 4. The panels show rank order plots of non-overlapping annual estimates of the (-) D_{ST} proxy based on averages of: (a) largest 0.5 % and (b) the largest 5 % of homogenized *aa*. The largest of these samples is plotted as rank 2, the next largest as rank 3 and so on. We plot as rank 1 two estimates of the Carrington event $D_{ST} = -850nT$ (red diamond) and $D_{ST} = -1760nT$ (red square). The uncertainty in the first ranked sample is estimated for an underlying exponential distribution. The green line indicates an exponential fit to the largest 100 values.